In experimental practice with electrical resistors and amplifiers the $1/f^{\alpha}$ behavior has been observed to extend over more than six frequency decades with no noticeable flattening at low-frequency [64].

$1/f^{\alpha}$ spectra have been observed in nature in a wide variety of systems: electrocardiac waves [65], the variation of sea levels [66], tardiness at work [67], etc. An essential feature of $1/f^{\alpha}$ noise is that it exhibits self similarity, that is, if one magnifies both time and space with the appropriate factor, the noise pattern is indistinguishable from the original one. So the noise does not have a characteristic timescale or length scale. $1/f$ noise is often seen as a signature of the fractal character of nature.

In 1987, Bak et al. [68] proposed a model for a universal mechanism behind $1/f$ noise. In their landmark paper they illustrated the concept of "self-organized criticality" with a sandpile model. When a sandpile has an inclination steeper than a critical angle θ, avalanches will occur that bring the pile back to the critical angle. When sand is added to the pile in a random fashion, these avalanches do not exhibit a characteristic size, nor do they appear after regular time intervals. Instead, there are bigger avalanches that are relatively rare and smaller avalanches that occur more frequently. The size distribution follows a power law in the frequency f. For instance, in one day there can be one avalanche involving more than 1000 grains, 10 involving more than 100 grains, 100 avalanches involving more than 10 grains, and so on. The picture that emerges is one of a system that is sitting on the critical edge between two phases and is "organizing" avalanches to stay there [69]. The most commonly cited real-life example of self-organized criticality is the Gutenberg–Richter power law for earthquakes. It appears that every year, on average, there is one earthquake larger than magnitude 8, 10 earthquakes larger than magnitude 7, and 100 earthquakes larger than magnitude 6. Self-organized criticality is an attractive theory. It proposes a simple mechanism and predicts power laws that can be easily verified or falsified. It has been utilized in a wide variety of contexts [69]. It has, for instance, been applied to evolutionary theory [70] and has been used to explain frequency-size distributions of forest fires [71].

How truly universally applicable self-organized criticality is and to what extent its claims may be unwarranted are matters that are still very much under debate. The $1/f$ proportionality for earthquakes applies only between magnitudes 5 and 8. Even for the archetypal sandpile, things turn out to be more involved upon close inspection than self-organized criticality suggests. Accurate measurements [72–74] on real sandpiles showed that in many cases there is no $1/f$ pattern in the avalanches. It turns out that system parameters, like the grain size and the rate of sand addition, determine to a large extent what kind of spectrum eventually emerges. The entire concept of self-organized criticality collapses, of course, if fine tuning by the experimentalist is crucial for the $1/f$ spectrum to materialize. All in all, $1/f$ noise is not as universal as first thought, and the dynamics behind nonequilibrium noise are usually best unraveled with *ad hoc* models.

The node of Ranvier is where the action potential for myelinated nerve cells is generated [75]. There is a high concentration of ion channels in the node of Ranvier, and in the days before patch clamp, it was a good place to record membrane electrical activity. In the mid-1960s, Verveen and Derksen measured 5–10 min of cell membrane voltage noise at a Ranvier node of an unstimulated nerve cell [76,77]. The resulting power spectrum showed two decades, between 10 Hz and 1000 Hz, of $1/f$ noise (see Figure 7.5). This $1/f$ noise, they found, was much larger in magnitude than what Nyquist's $4kTR$ formula (cf. Equation 7.5) would predict. Following the explanation for $1/f$ noise in ordinary resistors (cf. Equation 7.10 and Equation 7.11), Verveen and Derksen suggested that an ion channel could, from time to time, get "clogged up." The wide distribution of waiting times (i.e., the λs in Equation 7.8 through Equation 7.11) before getting unclogged would then give rise to the $1/f$ spectrum [78].

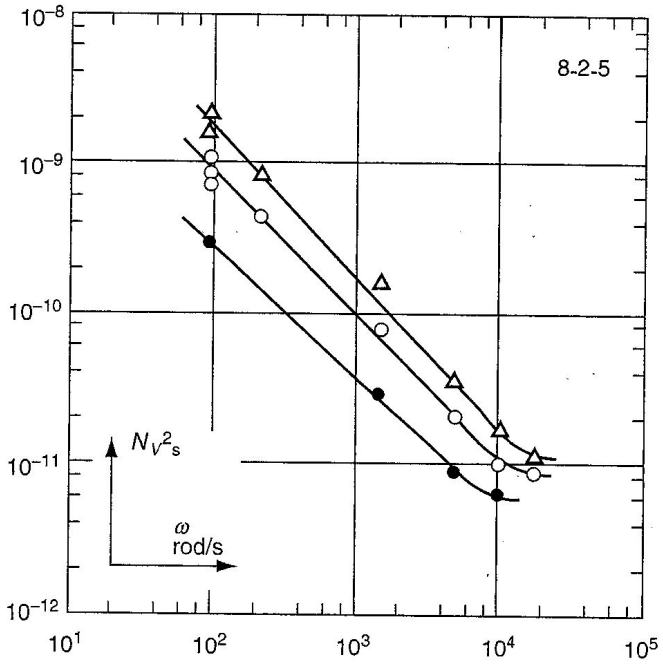

FIGURE 7.5
The voltage noise spectral densities from the frog node of Ranvier at room temperature at rest (open circles), at 10-mV depolarization (open triangles), and at 10-mV hyperpolarization (filled circles) [76,77]. (© Dutch Physiological Society. With permission.)

In the last two decades, single-channel recordings have shown how, even without stimulus, ion channels open and close repeatedly [40,75]. The kinetics behind the openings and closings is still very much a matter of debate. Modeling an ion channel as a two-state molecule with an open and a closed state and chemical steps with constant rates connecting these states appears not to account for the data in many cases. Electrophysiologists have commonly resorted to explaining the nonexponential distributions of open and closed times with a kinetic scheme that contains more than two states. With such an approach any distribution of open and closed times can always be fitted with a kinetic scheme [79–81]. It is just a matter of coming up with sufficiently many parameters (i.e., states and rates) to fit the data. In chemical kinetics the transitions are always assumed to be Markov transitions, that is, the probability of moving from a state 1 to a state 2 is constant and does not depend on the time that the molecule has been in state 1. A channel that is making such Markov transitions between a finite number of states always exhibits a power density spectrum that is a sum of Lorentzians. The number of characteristic times in the spectrum will always be one less than the number of states. If the characteristic times are sufficiently far apart, the power density spectrum will exhibit a number of identifiable plateaus when plotted on the customary logarithmic scale. The inflection points between the plateaus occur at the inverses of the characteristic times.

An alternative approach, foreshadowed by the aforementioned suggestion of Verveen and Derksen, has been to model the open to closed transition rates of an ion channel as time dependent, for instance $k(t) \propto t^{-\mu}$, where $0 < \mu < 1$ [82–85]. The exponent μ is taken to be smaller than unity to make $\int_\tau^\infty k(t)\, dt$ diverge for all $\tau > 0$ and thus guarantee the inevitability of an eventual transition. The proportionality $k(t) \propto t^{-\mu}$ leads to a decreasing transition probability, that is, the channel is "stabilizing in its openess," as more time is spent in the open state. There is ample justification for the use of open–closed transition rates that vary in time. A protein has many degrees of freedom and is subject to many equilibrium and nonequilibrium fluctuations. If an intramolecular rearrangement, like a transition between an open and a closed state, can be modeled as the crossing of an

activation barrier, then that barrier will most likely not be fixed and stationary. A fluctuating barrier implies fluctuating open–closed transition rates. We could thus get the infinitely many relaxation rates that give rise to the $1/f$ power density spectra of Equation 7.10 and Equation 7.11. Under physiological conditions an ion channel is trafficking ions in an electric field of tens of megavolts per meter and comparable chemical gradients. This is a very nonequilibrium setup, and it has been conjectured that the channel operates as a self-organized critical structure. One authoritative textbook [65] states it as follows:

> A channel protein may be a self-organizing critical system. The channel protein consists of many pieces that interact with their neighbors. The energy added to the protein from the environment causes local strains that are spread throughout the structure. If these distortions spread faster than the time it takes for the structure to thermally relax, then the channel protein may be a self organizing critical system. If that is the case, then the fluctuations in the channel structure will be due to a global organization of the local interactions between many small interacting pieces of the channel protein. The fractal scaling would then be due to the fact the channel structure is poised at a phase transition between its open and closed conformational shapes.

Over the past few years increasing amounts of data have been gathered with ever more accurate technology. Recently, the $1/f$ power spectral density of a nerve cell that Verveen and Derksen discovered was more accurately rerecorded [86]. But through careful subsequent experimentation and computer simulations, these researchers were also able to show how the apparent $1/f$ result comes about as the sum of a number of Lorentzian contributions. Each type of channel has its own Lorentzian, and because of close characteristic times the sum of the individual sigmoids appears like a smoothly decreasing $1/f$ curve.

For a single channel, things often turn out to be much more intricate than simple $1/f$ versus Markov kinetics. In single-channel recordings of a bacterial ion channel it was found that actual channel openings and closings follow Markov kinetics and lead to Lorentzian contributions to the ultimate net power spectrum [87]. The $1/f$ noise that is present in the power spectrum originates from transitions between open states of a slightly different (about 1–5%) conductance. The rates of these miniconductance transitions appeared to be independent of the transmembrane voltage. The small transitions in conductance have been conjectured to be due to small clusters within the channel's structure moving in and out of the lining of the pore [87]. A cluster can cause a partial flow constriction when it sticks out into the pore. Following this idea, the apparent $1/f$ behavior can be attributed to many different clusters moving in and out with equally many different relaxation times. The voltage independence comes about because these clusters are either uncharged or the external electric field is somehow screened. Noise in synthetic channels has also been studied [88]. There it was found that potassium currents through a one-state, permanently open channel exhibit $1/f^2$ noise. An artificial channel that can open and close, on the other hand, was found to exhibit $1/f$ noise when the externally applied voltage is in the right regime. With this latter artificial channel there is good ground to attribute the open–closed transitions to the movement of "dangling ends" of polymers in the pore's lining. So the result supports the "moving cluster" for the mechanism behind $1/f$ noise in channels.

There appears to be no simple theory that can convincingly bring all manifestations of $1/f$ noise under one common denominator. All the indications are that an *ad hoc* approach to nonequilibrium noise phenomena is still the most fruitful one.

In ordinary resistors the amount of $1/f$ noise grows linearly with the dissipated power W. If we take $S(\omega)\,d\omega$ to denote the power in energy per unit of time (watts) in an interval $d\omega$, then we have for the power spectral density:

$$S(\omega) = \frac{gW}{f} \tag{7.12}$$

Here, g is a dimensionless constant the value of which depends on the type of resistor.

Nyquist noise is simple in that the net value of the resistance R fully determines the noise amplitude. With $1/f$ noise a more complex situation arises. Experimentally, the constant g (cf. Equation 7.12) turns out to be proportional to the volume-to-power ratio [89]. In Figure 7.6 the four resistors in design (b) are identical to the one resistor in design (a). It is obvious that (a) and (b) will have the same net resistance and therefore the same amount of Nyquist noise. Design (a), however, will exhibit four times as much $1/f$ noise as design (b). Design (b) is quieter because the energy dissipation is distributed over a larger volume. Generally, we have $g \propto 1/V$, where V denotes the resistor's volume. The gW in Equation 7.12 can be expressed as $g_e w$, where g_e is the g-value for a single elementary charge carrier in the resistor and w is the energy dissipated in the volume of such a single, independent charge carrier.

Pumps and carriers move ions one by one. Imagine a single pump or carrier that moves ions across the membrane at a rate ν. During a small time interval dt there is a probability $p = \nu\,dt$ that an ion is transported. We take dt to be sufficiently small so that the probability of more than one ion being transported during dt is negligible. We also take the duration of the catalytic cycle, that is, the "processing" time for an ion going through the membrane, to be negligible in comparison to the time between catalytic cycles. If we were not to make the latter assumption, we would simply have to multiply by the probability that an average channel is available for transport when we want to express the transport rate. For the average number of ions $\langle n\rangle_{dt}$ transported by the channel in time dt, we now have $\langle n\rangle_{dt} = 1 \cdot p + 0 \cdot (1-p) = p$. For the variance we have $\sigma_{dt} = \langle n^2\rangle - \langle n\rangle^2 = 1^2 \cdot p - (1 \cdot p)^2 = p(1-p)$. For M subsequent timesteps and $M\,dt = T$, the variances add up, and we have $\langle n\rangle_T = Mp$ and $\sigma_T = Mp(1-p)$. So the standard deviation, $\sqrt{\sigma_T}$, works out to be proportional to $\sqrt{M}$. Over time the standard deviation becomes more and more negligible compared to the average. For sufficiently small dt we can take $1 - p$ to be equal to 1, and we then have a variance that equals the average.

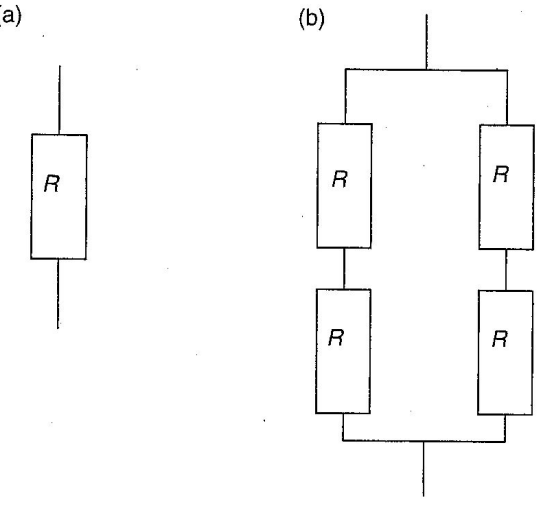

FIGURE 7.6
Design (a) and design (b) both have a net resistance R. They are different in that design (b) actually consists of two parallel resistors of $2R$. Designs (a) and (b) will exhibit the same amount of equilibrium noise, as it is only the net resistance (cf. Equation 7.5) that determines the equilibrium noise amplitude. It appears, however, that design (a) has four times as much power spectral density as design (b). The amount of nonequilibrium noise is proportional to the current density.

In the textbook by DeFelice [89] it is shown how the power spectral density of the process above amounts to $S(f) = 2\sigma_T/T = 2\nu$. The frequency-independent power spectrum can be intuited as follows. If the actual transport time through the membrane is small, then we can conceive of the transmembrane current as delta function-like pulses occurring at a rate ν. The Fourier transform of a Dirac delta function is a flat spectrum. In order to go from particle current to electrical current we must, to obtain the current power spectral density, multiply with the square of the charge of the involved ion. Taking this to be the elementary charge e, we find

$$S_i(f) = 2\nu e^2 = 2e\langle i\rangle \tag{7.13}$$

Here, $\langle i\rangle = e\nu$ denotes the average current through one pump.

Next, we let $\langle I\rangle$ denote the total transmembrane current due to pumps of a particular ion through the entire cell surface. We then have for the total current power spectral density:

$$S_I^{\text{pu}}(f) = 2e\langle I\rangle \tag{7.14}$$

For a living cell in a steady state, for each kind of ion, there are just as many ions going in as there are going out, that is, there is just as much uphill transport through pumps as there is downhill flow through ion channels. So we have the same current $\langle I\rangle$ uphill as well as downhill. Below, we will first show that the downhill flow through the channels generates much more nonequilibrium noise than the uphill flow through the pumps. We will then show how the channel noise far exceeds the Johnson–Nyquist equilibrium noise.

Ion channels stay open for an average time of about $\tau_{\text{op}} = 10^{-3}$ sec; and during that time there is a current of about 10^7 ions per sec (i.e., about 1 pA). So the equivalent of the elementary charge mentioned in the previous paragraph is now $N = 10^4$ ions.

However, before we blindly substitute Ne for e in Equation 7.14 to obtain the current power spectral density generated by the channel population of a cell, we have to take another source of variance into account. The channel-open time of about a millisecond is an average. If we view opening and closing of a channel as simple chemical steps between an open and a closed state, then the millisecond is the average of an exponential distribution of open times. For an exponential distribution the average open time equals the standard deviation in the open time. So the standard deviation ΔN equals N itself. The associated variance has to be added in. So we have $S_I^{\text{ch}}(f) \approx 2\,\nu e^2\,(N^2 + (\Delta N)^2)$. The rate ν now represents the number of channel openings per unit of time. So we get for the current power spectral density produced by the channels:

$$S_I^{\text{ch}} \approx 4Ne\langle I\rangle \tag{7.15}$$

So the channel contribution to the total nonequilibrium current noise is about 10^4 times as large as the contribution of the pumps. For the total current power spectral density, S_I^{noneq}, due to nonequilibrium currents, we thus neglect the pump contribution.

The above Equation 7.15 constitutes $S_I^{\text{ch}}(0)$. At higher frequencies, when f approaches the average open time τ_{op} of the channel, $S_I^{\text{ch}}(f)$ will decrease. The characteristic inverse time for a channel is $f_* = \tau_{\text{op}}^{-1} + \tau_{\text{cl}}^{-1}$, where τ_{cl} is the average closed time of the channel. With only one type of channel present in a cell, there will be a sigmoidally shaped, Lorentzian noise spectrum with an inflection point at $f = f_*$. With many types of channels for different kinds of ions present it is indeed possible to obtain a $1/f$ spectrum over several decades as the sum of Lorentzians [86].

To obtain the voltage power spectral density, we have to multiply $S_I^{\text{noneq}}(f)$ by R^2, where R represents the electrical resistance of the entire cell membrane. We let the cell surface area measure A. So we have $S_V^{\text{noneq}}(0) \approx 4\,Ne\,\langle I\rangle\,R^2$. The equilibrium Nyquist voltage noise across the same cell membrane is $S_V^{\text{eq}}(f) \approx 4kTR$. This is white noise and has the same strength at all frequencies. We thus obtain the following formula at $f = 0$ for the ratio $\theta(0)$ of the nonequilibrium noise and the equilibrium noise:

$$\theta(0) \approx \frac{Ne\langle I\rangle R}{kT} \tag{7.16}$$

The transmembrane current $\langle I\rangle$ is proportional to the cell surface A. The resistance R is inversely proportional to A. So eventually, the cell surface area and the cell geometry in general cancel out of the equation.

Data for the steady-state Na^+ flux through several types of cell membranes (e.g., rat soleus, sheep purkinje, squid axon, guinea pig auricles, and frog sartorius) are available [90]. That flux is about 50 pmol/(cm^2 sec). The vast majority of transmembrane ion transport is carried out by Na,K-ATPase, which transports two K^+ ions for every three Na^+ ions. We assume Na^+ and K^+ transport to therefore be about equal. After multiplying by Faraday's constant (the number of coulombs in a mole, i.e., about 10^5), we get a total current of about $\langle I\rangle \approx 10\ \mu$A/cm^2. The resistance of a cell membrane varies from 10^3 Ω cm^2 (squid axon) to 7×10^3 Ω cm^2 (mammalian cardiac cell). We thus find for $\theta(0)$ a value of about 5000.

Based on experimental data, it has been estimated that at 1 Hz the $1/f$ noise in the frog node of Ranvier is about a thousand times larger than thermal noise [91]. This is consistent with our estimate. Experimentally, it turns out that the power spectral density is constant from $f = 0$ up to about somewhere between 1 and 10 Hz [86,89]. At that point, the power spectral density starts to fall off as $1/f$. This means that we reach $\theta(f) = 1$, that is, the equilibrium and nonequilibrium noise being equal, somewhere near 10^4 Hz. Figure 7.5, in which the horizontal axis is in radians per second, indeed shows flattening between 10^3 and 10^4 Hz. At the 50- and 60-Hz power line frequencies, the nonequilibrium voltage noise is expected to exceed the equilibrium voltage noise by a factor of at least 10^2.

However, we should pause before taking the value of θ and employ it to incorporate nonequilibrium noise in the evaluation of a signal-to-noise ratio. As we saw earlier in this section, nonequilibrium noise may be a way to transduce energy from one stored form to another. So a signal can come in the form of a piece of nonequilibrium noise. With this gray area between signal and noise, it may no longer be straightforward to calculate a signal-to-noise ratio. There has been a natural selection toward high signal-to-noise ratios for signals whose detection has been important for the survival of the organism for many millennia. But what the signal-to-noise ratios and detection thresholds are for ELF and microwave radiation, which are relatively new phenomena in the environment, and how nonequilibrium noise figures in all of this is still open to conjecture and debate.

7.7 Chemical Noise

Chemical noise consists of both fundamental chemical noise (stochastic variations in net or accumulated amounts of a particular ion or molecule) and nonfundamental changes in chemical amount (molecular number) due to influences other than the applied field. We again adopt a recent discussion [12] in which an arbitrary biological system is considered.

In the discussion, attention focuses on weakly interacting fields that can create small chemical changes, but much of the approach is also relevant to strongly interacting fields, for example, those causing cell membrane electroporation (see Chapter 9 on electroporation in Ref. [127]). To begin, consider a small physical perturbation of the biological system due to the interaction of a local electromagnetic field, $\vec{F}_{\text{local}}(\vec{r}, t)$, that may vary from site to site within the volume of the biological system. In general, $\vec{F}_{\text{local}}$ may have a complicated dependence of its magnitude and direction on time and position, such that a formal prescription for calculating the field-induced molecular change due to an exposure is

$$\bar{n}_S = \int_{t=0}^{t=t_{\text{exp}}} \int_{\text{system volume}} J_0(t') f_{\text{bpm}}(\vec{F}_{\text{local}}(\vec{r},t'))\, dV\, dt' \tag{7.17}$$

We regard $\bar{n}_S$ as a molecular change signal. It is the primary consequence of the field exposure for the case where only one process, or one step in a cascade, is altered. Integration is carried out over the entire biological system volume and over the time comprising the exposure, t_{exp} (or control). This yields the accumulated, total chemical (molecular) change due to the applied field during the exposure. Other changes in the same ionic or molecular species may result from competing influences, for example, temperature variations, during t_{exp}.

The applied field interacts through one or more of a limited class of biophysical mechanisms. Here, *biophysical mechanism* means a class of interactions by which the field alters an ongoing biochemical rate (transport or reaction), with the rate arising from nonequilibrium processes dependent on metabolism. Examples of known biophysical mechanisms involving electric fields are heating (most biochemical processes have a nonzero temperature dependence), voltage-gated channels, electroconformational coupling of membrane enzymes, electroporation, and iontophoresis (mainly electrophoresis, but in some cases also electroosmosis). Examples involving magnetic fields are radical-pair reactions and twisting of magnetic material (magnetite or contaminant magnetic particles). As used here, a biophysical mechanism modulates an ongoing biochemical process, and both the coupling strength and the magnitude of the basal rate are important.

For a particular type of biophysical mechanism (bpm), the function $f_{\text{bpm}}(\vec{F}_{\text{local}}(t))$ describes the instantaneous alteration of the basal rate, J_0, which itself can vary in time [92]. The local field can be computed numerically at the tissue level (millimeter scale; see Chapter 11 on dosimetry, this volume) [93–99] and at the cellular level [100,101]. The time and position dependence of $\vec{F}_{\text{local}}(\vec{r},t)$ is often simple, namely, a constant magnitude (steady or DC) field, a constant amplitude periodic (AC) field, or at high frequencies a spatially decaying amplitude field due to power absorption. Environmental and occupational fields can be much more complicated, such that piecewise continuous representations may be needed.

If a weakly coupled physical perturbation alters the basal rate of a biochemical process (transport or reaction), the total chemical (molecular) change, expressed as the number of molecules, is

$$\bar{n} = \bar{n}_0 + \bar{n}_S \tag{7.18}$$

where $\bar{n}_0$ is the basal change during an exposure (sensing) time t_{exp}, and $\bar{n}_S$ is the (much smaller) molecular change due to the field exposure [22,45,92,102]. As noted above, $\bar{n}_S$ can be regarded as a molecular change signal. The basal process is far from equilibrium,

driven by free-energy differences associated with metabolism. The largest field-induced molecular change occurs for a steady (DC) field exposure [22,102]:

$$\bar{n}_S = K_{\text{bpm,dc}} F_0 \, J_0 \, t_{\text{exp}} \tag{7.19}$$

where $K_{\text{bpm,dc}}$ describes the alteration of the basal rate by the steady field, here of magnitude F_0. Equation 7.19 is the DC version of the case of a weakly coupled periodic perturbation, previously described for the case of an extracellular electric field [45,92], namely,

$$\bar{n}_S = K_{\text{bpm,ac}} F_0^2 \, J_0 \, t_{\text{exp}} \tag{7.20}$$

where $K_{\text{bpm,ac}}$ describes the coupling that leads to rectification of the ongoing rate [45]. For basal rates with more complicated time dependence, Equation 7.17 may need to be evaluated numerically, but the same basic ideas apply. Equation 7.20 is valid for long exposures, involving a large number of cycles of the periodic field. Basal rates that can be altered by weakly interacting electromagnetic fields by definition involve small interaction energies, so that thermal fluctuations and chemical free-energy differences result in nonzero basal rates. A zero basal rate with an extremely large activation or interaction energy cannot, therefore, be expected to be changed to a measurable nonzero rate by a weakly interacting field.

A generalized, molecular change-based signal-to-noise ratio can be constructed by estimating the ratio of primary molecular change to the combined competing changes for the same molecular (ionic) species. We consider the simplest case of the field altering the rate at one step in a single pathway but note that in principle the present analysis can be extended to include multiple steps involving more than one biochemical pathway. We further assume that this biochemical has its rate through the pathway altered slightly by a physical perturbation, here an electromagnetic field. But competing influences can also alter the rate. Such influences include temperature variations, normal physiological concentration variations, changes in hormones and other regulating biochemicals, and mechanical perturbations of cells and tissues. Competing molecular changes can also be created by a background electromagnetic field, for example, normal electrical activity within the human body or by movement in the earth's magnetic field, interacting through the same biophysical mechanism. Such competition goes beyond fundamental chemical noise (molecular shot noise). Nonionizing influences can only modulate ongoing processes, and therefore such influences cannot (essentially by definition) introduce foreign molecules. This has the important consequence that competing molecular changes may arise from several sources (Table 7.1).

TABLE 7.1

Quantities Employed in Generalized Chemical Noise

Symbol	Molecular Change	Source
S	$\bar{n}_S$	Field-induced molecular change signal
N	$\sqrt{\bar{n}} \approx \sqrt{\bar{n}_0}$	Molecular shot noise (fundamental)
V	$\bar{n}_V$	Molecular change due to temperature variations
C	$\bar{n}_C$	Molecular change due to concentration variations
I	$\bar{n}_M$	Molecular change due to mechanical interference
B	$\bar{n}_B$	Molecular change due to background fields

A generalized signal-to-noise ratio $(S/N)_{gen}$, can thus be considered. The field-induced molecular change signal, S, is thereby quantitatively compared to the several sources of competing molecular changes for the same biochemical (molecule or ion), yielding

$$(S/N)_{gen} = \frac{S}{f_{com}(N,V,C,I,B)} \tag{7.21}$$

The various competing molecular changes, which may or may not be independent, are combined to give the total competing molecular change, f_{com}. Important simplifications can be made if the various competing molecular changes can be approximated as independent and random around their mean values. In this case, f_{com} can be approximated as

$$f_{com}(N,V,C,I,B) \approx [N^2 + V^2 + C^2 + I^2 + B^2]^{1/2} \tag{7.22}$$

Alternatively, emphasizing the changes in terms of numbers of molecules,

$$f_{com}(N,V,C,I,B) \approx [\bar{n}_0 + (\Delta n_V)^2 + (\Delta n_C)^2 + (\Delta n_M)^2 + (\Delta n_B)^2]^{1/2} \tag{7.23}$$

All significant sources of competing molecular change are directly relevant.

Consistent with experimental treatment of errors as random, here we consider the special case that all the important competing molecular changes can be approximated as independent and random variations around their mean value, as this allows the competing changes to be added in quadrature (Equation 7.22). This leads to a general molecular change-based signal-to-noise ratio that involves Gaussian distributions, namely,

$$(S/N)_{gen} \approx \frac{S}{[N^2 + V^2 + C^2 + I^2 + B^2]^{1/2}} \tag{7.24}$$

Each of these competing molecular changes is discussed briefly below, with reference to Table 7.1.

As indicated in Table 7.1, $N = \sqrt{\bar{n}} \approx \sqrt{\bar{n}_0}$ is the competing molecular change due to fundamental stochastic variations in biochemical reaction and transport processes [15,45,92], which provides a fundamental, minimum molecular change noise. Fundamental chemical noise is increasingly recognized as important to understanding other aspects of biological systems, such as the circadian clock [103,104], control of genetic circuits [105,106], and bacterial chemotaxis [107].

Temperature variations within the volume of the biological system are generally expected to result in altered rates. When integrated over the system volume and over the exposure time, a contribution to the end-point molecular change is expected, because most biochemical processes have nonzero temperature dependence. Thus, $V = \bar{n}_v$ is the resulting, competing molecular change due to temperature variations [15]. Human core body temperature has daily variations of more than 1°C [108–113], and there are even larger variations in the extremities. Often *in vitro* electric and magnetic field experiments use feedback control, for instance, in temperature-regulated exposure chambers, but these typically have variations greater than about 0.01°C at one or a few temperature measurement sites. Temperature variations within the biological system itself are often inferred,

preferably by numerical models that can reasonably predict the temperature through the biological system by first predicting the specific absorption rate. During the exposure time, interfering temperature variation can be significant. To allow correction for temperature variations, the biological system should be characterized for its temperature sensitivity, and each particular apparatus should be characterized for its temperature variations for control and exposed conditions. As an example, an investigation first reporting athermal effects [114] was subsequently found to have temperature variation ~0.1°C at temperature measurement sites [115]. Without thermal modeling of the exposure systems and the biological systems, however, larger temperature changes away from the measurement site cannot be ruled out. It is the temperature change and variation over the entire volume containing cells (or other specimens) that need to be quantitatively understood. Temperature measurement at one site, typically somewhere along the perimeter or boundary of a temperature-regulated apparatus, is generally insufficient. The measured biochemical quantity should also be characterized for its temperature sensitivity for the biological system studied, so that the expected V can be determined, to address the basic specificity question of whether an observed change is due to the field or to temperature changes [116].

Changes in concentration of biochemicals involved in a process are well known to alter the rate of a process. Relevant chemical species include substrates, products, inhibitors, etc. The competing molecular change due to one or more interfering concentration changes is $C = \bar{n}_C$. In this case, a significant difference may exist for *in vitro* and *in vivo* experiments. Usually, only small, slow changes of chemical concentrations are expected *in vitro*, occurring, for example, through absorption or release of molecules (ions) from glass- and plasticware, spontaneous chemical decomposition, binding to cellular constituents, or evaporation. Uptake or release of interfering biochemicals from a biological preparation could be the predominant source, particularly if cells grow (taking up molecules) or die (releasing molecules). *In vivo* concentration variations are relatively large, because of normal physiologic variations. For example, Ca^{2+} concentration varies in humans by more than 1% over a day [117,118]. Unless buffered, these normal biochemical variations also compete with the field-induced molecular change.

Movement of tissue *in vivo* and vibration of an experimental apparatus containing a biological system can also create a mechanically induced molecular change, $I = \bar{n}_M$, that competes with a molecular change signal. In this case, the competing molecular change is due to interference of mechanical stress and strain [119,120], often present at high levels in living humans [11,121,122] but at low levels for *in vitro* experiments. *In vitro* apparatus can have quite different mechanical properties and isolation from ambient vibrations. Indeed, it has been found in some experiments that mechanical vibrations create effects larger than the field exposure [123]. Tissues *in vivo* experience significant mechanical deformation, but there is the least strain expected within the bone marrow and the brain [120]. This may be relevant to the "contact current hypothesis," which suggests that currents in the bone marrow may be important in exposures of children [124–126].

Background fields can, of course, also couple to biochemical processes through the same biophysical mechanisms as the applied field. Background field-induced molecular change competes, and is denoted by $B = \bar{n}_B$. Examples of background electromagnetic fields include the endogenous electrical fields generated within the body by cardiac, muscular, and neural activity and the sampling of different field values (local anomalies) in the ambient magnetic field as mobile humans move about in their environment. *In vitro* background fields will depend on the particular experimental environment, are usually small and constant, and are often measured.

7.8 Interpretation of Experiments

Specificity is fundamentally important to interpret experiments, as one wants to know what agent is responsible for the observed change(s). This is particularly relevant to experiments that find small changes in biological systems that are exposed to small electromagnetic fields. A basic challenge is to show that other influences are not responsible. Because it is well known that most biochemical processes have a significant temperature dependence, the approximate temperature sensitivity of the observed quantity should be determined or known, and some bound should be established for temperature drift or variations in the experiment. However, as already noted, even big changes can have more than one candidate cause. Both tissue electroporation and tissue movement can, for instance, underlie the changes in molecular uptake associated with large field pulses. For this reason, signal-to-noise ratio considerations should be preceeded by establishing field specificity, which can be much more difficult than observing a change associated with a field exposure. To establish specificity, a number of issues must be considered, many of which will be discussed next.

Many experiments determine quantities related to biochemical change. Exceptions are experiments that determine physical quantities such as voltages and currents, temperature changes, and magnetic particle rotation. However, electrical measurements are the most frequent physical measurement. These are incredibly important to systems of excitable cells, with experimental preparations ranging from isolated cells to electrophysiologic measurements on humans. Accumulation of charge might be measured, but probably as a voltage on a capacitance. Signal-to-noise ratio issues are still important, of course, but usually there is an important distinction: voltages and currents (rarely charge) are readily measured continuously.

A further distinction is that most experiments involving exposures to small fields use long exposure times (many seconds to hours or even days). Such experiments commonly determine biochemical quantities directly, for example, enzyme activity, or indirectly, for example, fluorescence emission from fluorescent indicators of intracellular calcium concentration. In this broad case, consideration of generalized chemical noise is relevant. Following the discussion in a recent paper [12], both the magnitude of the field perturbation and the nature and magnitude of chemical competition need to be understood. Such analysis should explicitly estimate the coupling to ongoing, far from equilibrium, metabolically driven biochemical processes and should quantitatively determine molecular changes due to competing influences. Only then can the analysis distinguish idealized conditions from *in vitro* conditions and *in vivo* conditions and then determine whether reported effects can be explained by known biophysical mechanisms.

In vivo there are several kinds of noise, and it is important to distinguish between them. Equilibrium noise comes about as a consequence of Brownian motion, that is, the random movement of molecules at finite temperature. At equilibrium, every degree of freedom takes on the same amount of energy, and equilibrium noise is therefore easy to evaluate. For a signal to exceed the equilibrium noise band, the quantitative criteria are often readily derived. Such baseline criteria can be useful when assessing the electroreception and magnetoreception that many organisms exhibit. But the nonequilibrium nature of life brings in nonequilibrium noise. When a primary molecular change is amplified through a biochemical cascade, "amplifier noise" is inevitable. Nonequilibrium noise appears whenever energy is dissipated, that is, when work is done. In many biological contexts the nonequilibrium noise is much more intense than the equilibrium noise. A serious complication is constituted by the fact that nonequilibrium noise, unlike equilibrium noise, is also able to perform work, that is, be a power source for an energetically uphill

process. Many biological processes may rely on the energy transduction that can be accomplished through nonequilibrium noise. The analysis of such situations poses challenges as the noise may be a signal and the signal may be noise. There is no easy general "common denominator" theory for nonequilibrium noise like there is for equilibrium kT-noise.

In a recent discussion [12], it is argued that experimental measurements can be plausibly related quantitatively to an underlying primary molecular change because of a field exposure operating through a biophysical mechanism. It is further argued that only the uncertainty in this change propagates through biochemical amplification and therefore dominates the measurement uncertainty. A more complete approach would involve traditional, independent determination of the instrumental or assay error (quantitative characterization of the experimental measurement system). After removal of the "instrumental noise," the generalized signal-to-noise ratio $(S/N)_{gen}$, could be revised upward. This would allow interpretation (correction) of experimental error to estimate the uncertainty in the measured quantity itself. Assessment of combinations of biophysical mechanism models and particular exposure can then be carried out, using the most field-sensitive versions of theoretical models for the candidate biophysical mechanisms. The criterion $(S/N)_{gen} \leq 0.1$ is a very conservative basis for ruling out a particular class of biophysical mechanism for a given field exposure. Similarly, the criterion $(S/N)_{gen} \geq 10$ is a conservative basis for ruling in a candidate biophysical mechanism for a given exposure, retaining that biophysical mechanism hypothesis for further evaluation. This approach provides a quantitative basis for rejecting or accepting hypothetical biophysical mechanisms as candidate explanations for an experimental measurement.

The traditional choice $(S/N)_{gen} \approx 1$ is a useful but somewhat arbitrary dividing line, which indicates conditions for which an effect might appear. $(S/N)_{gen} \leq 0.1$ and $(S/N)_{gen} \geq 10$ provide criteria for stronger conclusions, allowing rejection or provisional retention of a biophysical mechanism hypothesis. This approach to interpreting experiments thus provides a general method for carrying out theoretical assessment of reported weak field exposure effects. This approach can distinguish relatively quiet *in vitro* conditions from *in vivo* conditions containing more and larger influences of competing molecular change. This in turn allows quantitative estimates of whether an *in vitro* result is relevant to *in vivo* conditions.

Acknowledgment

This work was supported partially by NIH grant RO1-GM63857.

References

1. G.N. Stewart. The changes produced by the growth of bacteria in the molecular concentration and electrical conductivity of culture media. *J. Exp. Med.*, 4:235–243, 1899.
2. R. Eden and G. Eden. *Impedance Microbiology*. Research Studies Press, Letchworth, Herts, U.K., 1984.
3. M. Wawerla, A. Stolle, B. Schalch, and H. Eisgruber. Impedance microbiology: applications in food hygiene. *J. Food Prot.*, 62:1488–1496, 1999.

4. J. McPhillips and N. Snow. Studies on milk with a new type of conductivity cell. *Aust. J. Dairy Technol.*, 3:192–196, 1958.
5. T. Ritz, P. Thalau, J.B. Phillips, R. Wiltschko, and W. Wiltschko. Resonance effects indicate a radical-pair mechanism for avian magnetic compass. *Nature*, 429:177–180, 2004.
6. D. Cohen. Ferromagnetic contaminants in the lungs and other organs of the body. *Science*, 180:745–748, 1973.
7. J.L. Kirschvink, A.K. Kirschvink, and B.J. Woodford. Magnetite biomineralization in the human brain. *Proc. Natl. Acad. Sci.*, 89:7683–7687, 1992.
8. J.R. Dunn, M. Fuller, J. Zoeger, J. Dobson, F. Heller, J. Ilammann, E. Caine, and B.M. Moskowitz. Magnetic material in the human hippocampus. *Brain Res. Bull.*, 36:149–153, 1994.
9. P.L. McNeil and S. Ito. Molecular traffic through plasma membrane disruptions of cells. *In Vivo J. Cell Sci.*, 96:549–556, 1990.
10. P.L. McNeil and R.A. Steinhardt. Loss, restoration, and maintanence of plasma membrane integrity. *J. Cell Biol.*, 137:1–4, 1997.
11. P.L. McNeil and M. Terasaki. Coping with the inevitable: how cells repair a torn surface membrane. *Nat. Cell Biol.*, 3:124–129, 2001.
12. T.E. Vaughan and J.C. Weaver. Molecular change signal-to-noise criteria for interpreting experiments involving exposure of biological systems to weakly interacting electromagnetic fields. *Bioelectromagnetics*, 26:305–322, 2005.
13. N.G. Van Kampen. *Stochastic Processes in Physics and Chemistry*. Elsevier, Amsterdam, 1992.
14. R.C. Duncan, R.G. Knapp, and M.C. Miller. *Introductory Biostatistics for the Health Sciences*. John Wiley & Sons, New York, 1983.
15. J.C. Weaver, T.E. Vaughan, and G.T. Martin. Biological effects due to weak electric and magnetic fields: the temperature variation threshold. *Biophys. J.*, 76:3026–3030, 1999.
16. J.C. Weaver. Understanding conditions for which biological effects of nonionizing electromagnetic fields can be expected. *Bioelectrochemistry*, 56:207–209, 2002.
17. C.W. Helstrom. *Statistical Theory of Signal Detection*, Second Edition. Pergamon Press, New York, 1968.
18. A.J. Kalmijn. Electro-perception in sharks and rays. *Nature*, 212:1232–1233, 1966.
19. A.J. Kalmijn. Electric and magnetic field detection in elasmobranch fish. *Science*, 218:916–918, 1982.
20. W.J. Moore. *Physical Chemistry*. Longman, London, 1972.
21. A.J. Kalmijn. Graded positive feedback in elasmobranch ampullae of lorenzini. In S.M. Bezrukov, Ed. *Unsolved Problems of Noise and Fluctuations: UPoN 2002: Third International Conference*, volume 665 of *Conference Proceedings*, pp. 133–141, American Institute of Physics, Melville, NY, 2003.
22. R.K. Adair, R.D. Astumian, and J.C. Weaver. Detection of weak electric fields by sharks, rays, and skates. *Chaos*, 8:576–587, 1998.
23. S.M. Bezrukov. Sensing nature's electric fields: ion channels as active elements of linear amplification. In S.M. Bezrukov, Ed. *Unsolved Problems of Noise and Fluctuations: UPoN 2002: Third International Conference*, volume 665 of *Conference Proceedings*, pp. 142–149, American Institute of Physics, Melville, NY, 2003.
24. J.C. Weaver, T.E. Vaughan, and R.D. Astumian. Biological sensing of small field differences by magnetically sensitive chemical reactions. *Nature*, 405:707–709, 2000.
25. R.P. Blakemore. Magnetotactic bacteria. *Science*, 190:377–379, 1975.
26. R. Blakemore. Magnetotactic bacteria. *Annu. Rev. Microbiol.*, 36:217–238, 1982.
27. J.L. Kirschvink, M.M. Walker, and C.E. Diebel. Magnetite-based magnetoreception. *Curr. Opin. Neurobiol.*, 11:462–467, 2001.
28. J.L. Kirschvink. Comment on "Constraints on biological effects of weak exteremely-low-frequency electromagnetic fields." *Phys. Rev. A*, 46:2178–2184, 1992.
29. M.M. Walker, T.E. Dennis, and J.L. Kirschvink. The magnetic sense and its use in long-distance navigation by animals. *Curr. Opin. Neurobiol.*, 12:735–744, 2002.
30. National Institute of Environmental Health Sciences (NIEHS). NIEHS Report on Health Effects from Exposure Power-Line Frequency Electric and Magnetic Fields. NIH Publication No. 99–4493, 1999.

31. R.K. Adair. Effects of ELF magnetic fields on biological magnetite. *Bioelectromagnetics*, 14:1–4, 1993.
32. C. Polk. Effects of extremely-low-frequency magnetic fields on biological magnetite. *Bioelectromagnetics*, 15:261–270, 1994.
33. R.K. Adair. Constraints on biological effects of weak extremely-low-frequency electromagnetic fields. *Phys. Rev. A*, 43:1039–1048, 1991.
34. K.R. Foster and H.P. Schwan. Dielectric properties of tissues and biological materials: a critical review. *CRC Crit. Rev. Bioeng.*, 17:25–104, 1989.
35. J.B. Johnson. Thermal agitation of electricity in conductors. *Phys. Rev.*, 32:97–109, 1928.
36. H. Nyquist. Thermal agitation of electric charge in conductors. *Phys. Rev.*, 32:110–113, 1928.
37. W. Schottky. Über spontane stromschwankungen in verschiedenen elektrizitätsleitern. *Ann. Phys. (Leipzig)*, 57:541–568, 1918.
38. R. Sarpeshkar, T. Delbrück, and C.A. Mead. White noise in MOS transistors and resistors. *IEEE Circuits Devices*, Nov.:23–29, 1993.
39. M. Bier. Gauging the strength of power frequency fields against membrane electrical noise. *Bioelectromagnetics*, 26:595–609, 2005.
40. B. Hille. *Ion Channels of Excitable Membranes*. Sinauer, Sunderland, MA, 1992.
41. P. Läuger. *Electrogenic Ion Pumps*. Sinauer, Sunderland, MA, 1991.
42. J.C. Weaver and R.D. Astumian. The response of living cells to very weak electric fields, the thermal noise limit. *Science*, 247:459–462, 1990.
43. W.T. Kaune. Thermal noises limit on the sensitivity of cellular membranes to power frequency electric and magnetic fields. *Bioelectromagnetics*, 23:622–928, 2002.
44. G. Vincze, N. Szasz, and A. Szasz. On the thermal noise limit of cellular membranes. *Bioelectromagnetics*, 26:28–35, 2005.
45. R.D. Astumian, J.C. Weaver, and R.K. Adair. Rectification and signal averaging of weak electric fields by biological cells. *Proc. Natl. Acad. Sci.*, 92:3740–3743, 1995.
46. L. Brillouin. Can the rectifier become a thermodynamical demon? *Phys. Rev.*, 78:627–628, 1950.
47. P.W. Bridgman. Note on the principle of detailed balancing. *Phys. Rev.*, 31:101–102, 1928.
48. R.C. Tolman. The principle of microscopic reversibility. *Proc. Natl. Acad. Sci.*, 11:436–439, 1925.
49. R.P. Feynman, R.B. Leighton, and M. Sands. *The Feynman Lectures on Physics*. Addison-Wesley, Reading, MA, 1966.
50. M. von Smoluchowski. Experimentell nachweisbare, der üblichen thermodynamik widersprechende molekularphänomene. *Phys. Zeitschr.*, 13:1069–1080, 1912.
51. P.W. Atkins. *The Second Law*. Scientific American Books, New York, 1984.
52. H.S. Leff and A.F. Rex, Eds. *Maxwell's Demon: Entropy, Information, Computing*. Princeton University Press, Princeton, NJ, 1990.
53. J. Howard and A.J. Hudspeth. Compliance of the hair bundle associated with gating of mechanoelectrical transduction channels in the bullfrog's saccular hair cell. *Neuron*, 1:189–199, 1988.
54. M. Magnasco. Forced thermal ratchets. *Phys. Rev. Lett.*, 71:1477–1480, 1993.
55. M. Bier. Brownian ratchets in physics and biology. *Contemp. Phys.*, 38:371–379, 1997.
56. R.D. Astumian and M. Bier. Fluctuation driven ratchets: molecular motors. *Phys. Rev. Lett.*, 72:1766–1769, 1994.
57. R.D. Astumian. Thermodynamics and kinetics of a brownian motor. *Science*, 276:917–922, 1997.
58. M. Bier and R.D. Astumian. Biased Brownian motion as the operating principle for microscopic engines. *Bioelectrochem. Bioenerg.*, 39:67–75, 1996.
59. I. Kosztin and K. Schulten. Fluctuation-driven molecular transport through an asymmetric membrane channel. *Phys. Rev. Lett.*, 93:238102-1–238102-4, 2004.
60. Z. Siwy, I.D. Kosińska, and A. Fuliński. On the validity of continuous modelling of ion transport through nanochannels. *Europhys. Lett.*, 67:683–689, 2004.
61. Z. Siwy, I.D. Kosińska, A. Fuliński, and C.R. Martin. Asymmetric diffusion through synthetic nanopores. *Phys. Rev. Lett.*, 94:048102-1–048102-4, 2005.
62. Z. Siwy and A. Fuliński. Fabrication of a synthetic nanopore ion pump. *Phys. Rev. Lett.*, 89:198103-1–198103-4, 2002.

63. J. Bernamont. Fluctuations in the resistance of thin films. *Proc. Phys. Soc.*, 49:138–139, 1937.
64. B. Pellegrini, R. Saletti, P. Terreni, and M. Prudenziati. $1/f^{\gamma}$ noise in thick-film resistors as an effect of tunnel and thermally activated emissions, from measures versus frequency and temperature. *Phys. Rev. B*, 27:1233–1243, 1983.
65. J.B. Bassingthwaighte, L.S. Liebovitch, and B.J. West. *Fractal Physiology*. Oxford University Press, New York, 1994.
66. C. Wunsch. Bermuda sea level in relation to tides, weather, and baroclinic fluctuations. *Rev. Geophys.*, 10:1–49, 1972.
67. M. Dishon-Berkovits and R. Berkovits. Work-related tardiness: lateness incident distribution and long-range correlations. *Fractals*, 5:321–324, 1997.
68. P. Bak, C. Tang, and K. Wiesenfeld. Self-organized criticality: an explanation of $1/f$ noise. *Phys. Rev. Lett.*, 59:381–384, 1987.
69. P. Bak. *How Nature Works*. Springer-Verlag, New York, 1996.
70. S. Kauffman. *Investigations*. Oxford University Press, New York, 2000.
71. B.D. Malamud, G. Morein, and D.L. Turcotte. Forest fires: an example of self-organized critical behavior. *Science*, 281:1840–1842, 1998.
72. H.M. Jaeger, C. Liu, and S.R. Nagel. Relaxation at the angle of repose. *Phys. Rev. Lett.*, 62:40–43, 1989.
73. S. Nagel. Instabilities in a sandpile. *Rev. Mod. Phys.*, 64:321–325, 1992.
74. M. Bretz, J.B. Cunningham, P.L. Kurczynski, and F. Nori. Imaging of avalanches in granular materials. *Phys. Rev. Lett.*, 69:2431–2434, 1992.
75. J.G. Nicholis, A.R. Martin, and B.G. Wallace, Eds. *From Neuron to Brain*. Sinauer, Sunderland, MA, 1992.
76. H.E. Derksen and A.A. Verveen. Fluctuations of resting neural membrane potential. *Science*, 151:1388–1389, 1966.
77. H.E. Derksen. Axon membrane voltage fluctuations. *Acta Physiol. Pharmacol. Neerl.*, 13:373–466, 1965.
78. H.E. Derksen and A.A. Verveen. Fluctuations in membrane potential of axons and the problem of coding. *Kybernetik* 2:152–160, 1965.
79. D. Colquhoun and A.G. Hawkes. On the stochastic properties of bursts of single ion channel openings and of clusters of bursts. *Philos. Trans. R. Soc. Lond.*, 300:1–59, 1982.
80. S.D. Silberberg and K.L. Magleby. Preventing errors when estimating single channel properties from the analysis of current fluctuations. *Biophys. J.*, 65:1570–1584, 1993.
81. D. Colquhoun, C. Hatton, and A.G. Hawkes. The quality of maximum likelihood estimation of ion channel rate constants. *J. Physiol. (Lond.)*, 547:699–728, 2003.
82. L.S. Liebovitch, J. Fishbarg, and J.P. Koniarek. Ion channel kinetics: a model based on fractal scaling rather than multistate Markov processes. *Math. Biosci.*, 84:37–68, 1987.
83. L.S. Liebovitch. Analysis of fractal ion channel gating kinetics: kinetic rates, energy levels, and activation energies. *Math. Biosci.*, 93:97–115, 1989.
84. L.S. Liebovitch. Testing fractal and Markov models of ion channel kinetics. *Biophys. J.*, 55:373–385, 1989.
85. I. Goychuk and P. Hänggi. Fractional diffusion modeling of ion channel gating. *Phys. Rev. E*, 70:051915-1–051915-9, 2004.
86. K. Diba, H.A. Lester, and C. Koch. Intrinsic noise in cultured hippocampal neurons: experiment and modeling. *J. Neurosci.*, 24:9723–9733, 2004.
87. S.M. Bezrukov and M. Winterhalter. Examining noise sources at the single molecule level: $1/f$ noise of an open maltoporin channel. *Phys. Rev. Lett.*, 85:202–205, 2002.
88. Z. Siwy and A. Fuliński. Origin of $1/f^{\alpha}$ noise in membrane channel currents. *Phys. Rev. Lett.*, 89:158101-1–158101-4, 2002.
89. L.J. DeFelice. *Introduction to Membrane Noise*. Plenum Press, New York, 1981.
90. O.M. Sejersted. Maintenance of Na,K-homeostasis by Na,K-pumps in striated muscle. *Prog. Clin. Biol. Res.*, 268B:195–206, 1988.
91. F.S. Barnes. Interaction of DC and ELF electric fields with biological materials and systems. In C. Polk and E. Postow, Eds. *Handbook of Biological Effects of Electromagnetic Fields*, pp. 103–147, CRC Press, Boca Raton, FL, 1996.

92. J.C. Weaver, T.E. Vaughan, R.K. Adair, and R.D. Astumian. Theoretical limits on the threshold for the response of long cells to weak ELF electric fields due to ionic and molecular flux rectification. *Biophys. J.*, 75:2251–2254, 1998.
93. M. Stuchly and T. Dawson. Interaction of low-frequency electric and magnetic fields with the human body. *Proc. IEEE*, 88:643–662, 2000.
94. M.A. Stuchly and O.P. Gandhi. Inter-laboratory comparison of numerical dosimetry for human exposure to 60 Hz electric and magnetic fields. *Bioelectromagnetics*, 21:167–174, 2000.
95. P.A. Mason, W.D. Hurt, T.J. Walters, J.A. D'Andrea, P. Gajšek, K.I. Ryan, D.A. Nelson, K.I. Smith, and J.M. Ziriax. Effects of frequency, permittivity and voxel size on predicted specific absorption rate values in biological tissue during electromagnetic-field exposure. *IEEE Trans. Microwave Theory Technol.*, 48:2050–2058, 2000.
96. P. Gajsek, T.J. Walters, W.D. Hurt, D.A. Nelson, and P.A. Mason. Empirical validation of SAR values predicted by FDTD modeling. *Bioelectromagnetics*, 23:37–48, 2002.
97. M. Nadeem, T. Thorlin, O.P. Gandhi, and M. Persson. Computation of electric and magnetic stimulation in human head using the 3-D impedance method. *IEEE Trans. Biomed. Eng.*, 50:900–907, 2003.
98. T.W. Dawson, K. Caputa, M.A. Stuchly, and R. Kavet. Comparison of electric fields induced in humans and rodents by 60-Hz contact currents. *IEEE Trans. Biomed. Eng.*, 50:744–753, 2003.
99. S.J. Allen, E.R. Adair, K.S. Mylacraine, W. Hurt, and J. Ziriax. Empirical and theoretical dosimetry in support of whole body radio frequency (RF) exposure in seated human volunteers at 220 MHz. *Bioelectromagnetics*, 26:440–447, 2005.
100. T.R. Gowrishankar and J.C. Weaver. An approach to electrical modeling of single and multiple cells. *Proc. Natl. Acad. Sci.*, 100:3203–3208, 2003.
101. D.A. Stewart, T.R. Gowrishankar, and J.C. Weaver. Transport lattice approach to describing cell electroporation: use of a local asymptotic model. *IEEE Trans. Plasma Sci*, 32:1696–1708, 2004.
102. P.C. Gailey. Membrane potential and time required for detection of weak signals by voltage-gated ion channels. *Bioelectromagnetics*, 20:102–109, 1999.
103. N. Barkai and S. Liebler. Circadian clocks limited by noise. *Nature*, 403:267–268, 2000.
104. M.B. Elowitz and S. Leibler. A synthetic oscillatory network. *Nature*, 403:335–338, 2000.
105. T.S. Gardner, C.R. Cantor, and J.J. Collins. Construction of a genetic toggle switch in *Escherichia coli*. *Nature*, 403:339–342, 2000.
106. A. Becskei and L. Serrano. Engineering stability in gene networks by autoregulation. *Nature*, 405:590–593, 2000.
107. T.S. Shimizu, S.V. Aksenov, and D. Bray. A spatially extended stochastic model of the bacterial chemotaxis signalling pathway. *J. Mol. Biol.*, 329:291–309, 2003.
108. H.T. Hammel. Regulation of internal body temperature. *Annu. Rev. Physiol.*, 30:641–710, 1968.
109. S.A. Rubin. Core temperature regulation of heart rate during exercise in humans. *J. Appl. Physiol.*, 62:1997–2002, 1987.
110. W.R. Keatinge, A.C. Mason, C.E. Millard, and C.G. Newstead. Effects of fluctuating skin temperature on thermoregulatory responses in man. *J. Physiol.*, 378:241–252, 1986.
111. K. Shiraki, S. Sagawa, F. Tajima, A. Yokota, M. Hashimoto, and G.L. Brengelmann. Independence of brain and tympanic temperatures in an unanesthetized human. *J. Appl. Physiol.*, 65:482–486, 1988.
112. P. Webb. Temperatures of skin, subcutaneous tissue, muscle and core in resting men in cold, comfortable and hot conditions. *Eur. J. Appl. Physiol.*, 64:471–476, 1992.
113. R.K. Adair. Biophysical limits on athermal effects of RF and microwave radiation. *Bioelectromagnetics*, 24:39–48, 2003.
114. D. de Pomerai, C. Daniells, H. David, J. Allan, I. Duce, M. Mutwakil, D. Thomas, P. Sewell, J. Tattersall, D. Jones, and P. Candido. Non–thermal heat-shock response to microwaves. *Nature*, 405:417–418, 2000.
115. D.I. de Pomerai, B. Smith, A. Dawe, K. North, T. Smith, D.B. Archer, I.R. Duce, D. Jones, and E.P.M. Candido. Microwave radiation can alter protein conformation without bulk heating. *FEBS Lett.*, 543:93–97, 2003.

116. Y.L. Zhao, P.G. Johnson, G.P. Jahreis, and S.W. Hui. Increased DNA synthesis in INIT/10$T_{1/2}$ cells after exposure to a 60 Hz magnetic field: a magnetic-field or a thermal effect? *Radiat. Res.*, 151:201–208, 1999.
117. B. Morrison, A. Shenkin, A. McLelland, D.A. Robertson, M. Barrowman, S. Graham, G. Wuga, and K.J. Cunningham. Intra-individual variation in commonly analyzed scrum constituents. *Clin. Chem.*, 25:1799–1805, 1979.
118. M.G. Weyer and H. Lommel. *LONG I: Eine Longitudinal-Studie über individuelle Normbereiche, individuelle Standardbereiche, statislische Normbereiche für Prävention und Früherkennung*. Verlag Kirchheim, Mainz, 1981.
119. T.E. Vaughan and J.C. Weaver. Energetic constraints on the creation of cell membrane pores by magnetic particles. *Biophys. J.*, 71:616–622, 1996.
120. T.E. Vaughan and J.C. Weaver. Molecular change due to biomagnetic stimulation and transient magnetic fields: mechanical interference constraints on possible effects by cell membrane pore creation via magnetic particles. *Bioelectrochem. Bioenerg.*, 46:121–128, 1998.
121. P.L. McNeil. Cell wounding and healing. *Am. Sci.*, 79:222–235, 1991.
122. D. Bansal, K. Miyake, S.S. Vogel, S. Groh, C.C. Chen, R. Williamson, P.L. McNeil, and K.P. Cambell. Defective membrane repair in dysferlin-deficient muscular dystrophy. *Nature*, 423:129–131, 2003.
123. U. Valtersson, K. Hanssson Mild, and M.-O. Mattsson. Uncharacterized physical parameters can contribute more than magnetic field exposure to ODC activity *in vitro*. In F. Bersani, Ed. *Electricity and Magnetism in Biology and Medicine*, pp. 449–452, Plenum Press, New York, 1999.
124. R. Kavet, L. Zaffanella, J. Daigle, and K. Ebi. The possible role of contact current in cancer risk associated with residential magnetic fields. *Bioelectromagnetics*, 21:538–553, 2000.
125. R. Kavet, L.E. Zaffenella, R.L. Pearson, and J. Dallaplazza. Association of residential magnetic fields with contact voltages. *Bioelectromagnetics*, 25:530–536, 2004.
126. R. Kavet. Contact current hypothesis: summary of results to date. *Bioelectromagnetics*, suppl. 7:S75–S85, in press.
127. J.C. Weaver, Y. Chizmadzhev, Electroporation. In F.S. Barnes and B. Greenebaum, *Biological and Medical Aspects*, Eds. Taylor & Francis, Boca Raton, FL, Chapter 9, 2006.